Title
Laser induced shockwave paired with FRET to study neuronal responses to shear stress

ISBN
9781510644342

Authors
Godinez, Veronica Gomez
Morar, Vikash
Carmona, Christopher
et al.

Publication Date
2021-08-03

DOI
10.1117/12.2595803

PROCEEDINGS OF SPIE

SPIEDigitalLibrary.org/conference-proceedings-of-spie

Laser induced shockwave paired with FRET to study neuronal responses to shear stress

Veronica Gomez Godinez, Vikash Morar, Christopher Carmona, Yingli Gu, Kijung Sung, et al.

Veronica Gomez Godinez, Vikash Morar, Christopher Carmona, Yingli Gu, Kijung Sung, Linda Z. Shi, Chengbiao Wu, Daryl Preece, Michael W. Berns, "Laser induced shockwave paired with FRET to study neuronal responses to shear stress," Proc. SPIE 11798, Optical Trapping and Optical Micromanipulation XVIII, 117982H (3 August 2021); doi: 10.1117/12.2595803

SPIE.

Event: SPIE Nanoscience + Engineering, 2021, San Diego, California, United States

Laser induced shockwave paired with FRET to study neuronal responses to shear stress.

Veronica Gomez Godinez*[a], Vikash Morar[a], Christopher Carmona[a], Yingli Gu[b], Kijung Sung[b], Linda Shi[q], Chengbiao Wu[b], Daryl Preece [c,d], Michael W. Berns[c,d,]
[a]Institute of Engineering in Medicine, University of California, San Diego, San Diego, California, United States of America. [b] Department of Neurosciences, University of California, San Diego, San Diego, California, United States of America.[c]Beckman Laser Institute and Medical Clinic, University of California, Irvine, United States of America. [d]Department of Biomedical Engineering, University of California, Irvine, Irvine, California, United States of America

ABSTRACT

Laser induced shockwave (LIS) can be utilized to subject neuronal cells to conditions similar to those occurring during a blast induced traumatic brain injury. We utilized a 532nm Coherent Flare laser to induce a shockwave near cells which had been transfected with a FRET calcium biosensor (D3CPV) so that we could monitor the immediate cellular responses. Our shockwave system was characterized with a high-speed camera to monitor cavitation bubble dynamics and calculate the shear forces cells were subjected to. We found that we could induce forces which have been previously shown to induce injury. Using both phase and fluorescence microscopy we monitored the effects of shear on our cells. We found that at distances up to 120 microns from the laser focal point cells experienced shears greater than 10kPa. At those distances cell fragmentation was observed. Cells that survived and expressed the FRET biosensor demonstrated an immediate calcium elevation irrespective of extracellular or cytoplasmic calcium concentration. Cells recovered to pre-shockwave calcium levels within ~30s. In conclusion, LIS can be utilized to simultaneously monitor the neuronal response to shear stress and nearby cell death or injury.

Keywords: Laser Induced Shockwave (LIS), Traumatic Brain Injury (TBI), D3CPV Calcium Biosensor, Neurons, Dorsal Root Ganglion DRG).

1. INTRODUCTION

Understanding the molecular mechanisms that occur in brain cells following a blast-induced traumatic brain injury (TBI) may help us identify ways to assess the level of damage or mitigate secondary effects. We utilized a laser induced shockwave (LIS) system to subject neuronal cells to shear stress similar to that which may induce a traumatic brain injury. The D3CPV calcium biosensor was transfected into neuronal cells so that we could monitor the calcium response. Cells demonstrated an immediate calcium elevation in response to LIS irrespective of extracellular calcium conditions. We found that LIS is a useful tool to investigate the molecular cascades which may be triggered immediately after TBI.

A shockwave is generated when the buildup of energy at the laser focus point leads to the formation of a cavitation bubble. The expansion of the cavitation bubble leads to a shockwave which extends beyond the bubble[1]. The shockwave can exert pressures on nearby cells. Previous studies have shown that bubble size is dependent on laser irradiance[2]. Therefore, the ability to modulate the laser power and location permits the user to have spatiotemporal control on the amount of pressure a cell may experience. As a result, one can monitor the cellular response to different shear stresses.

Ca^{2+} signaling is critical for neurotransmission, gene transcription, muscle contraction, cell motility and cell proliferation[3]. Ca^{2+} levels have been shown to be disrupted in the brain and blood serum of patients with a TBI[4]. Several studies have demonstrated the ability of LIS to stimulate a Ca^{2+} increase in the cytosol of various cell types: olfactory, drosophila epithelial, bladder carcinoma, bovine arterial endothelia, and human umbilical vein endothelial[5-9]. We demonstrate in this paper that cerebral cortex neurons undergo a cytosolic Ca^{2+} increase in response to LIS. To

Optical Trapping and Optical Micromanipulation XVIII, edited by Kishan Dholakia, Gabriel C. Spalding,
Proc. of SPIE Vol. 11798, 117982H · © 2021 SPIE · CCC code: 0277-786X/21/$21 · doi: 10.1117/12.2595803

monitor Ca^{2+} we transfected cells with a genetically encoded FRET biosensor (D3CPV). Upon Ca^{2+} binding the biosensor changes confirmation which leads to an increase in fluorescence intensity in the CPV(FRET) channel and a decrease in the ECFP channel[10].

2. METHODOLOGY

2.1 Shockwave System.

A 532nm Coherent Flare laser (Spectra-Physics, Mountain View, CA) was used to induce a shockwave. The power was attenuated by rotating an optical polarizer mounted on a stepper motor (Newport, Irvine, CA). The number of pulses entering the microscope was controlled by the use of a mechanical shutter with a 10-15ms duty cycle (Vincent Associates, Rochester, NY). The laser beam diameter was adjusted to fill the back aperture of a 40x NA 1.3 Zeiss objective. Prior to firing the laser, the objective was moved in the Z-direction so that the focus was 10μm above the substrate. The power before the objective was found to be 200-220μW. For fluorescence imaging, a Zeiss filter set 48 without the emission filter was mounted to the filter turret of the microscope. A band pass filter for FRET signal (535/30nm) and ECFP(480/40) were mounted on a LUDL filter wheel positioned before an ORCA-Flash 4.0 V2 Digital Hamamatsu CMOS camera.

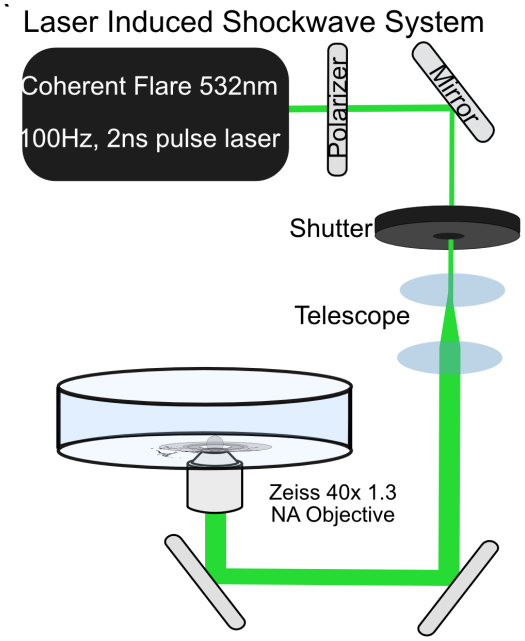

Figure 1. Laser set up for LIS. A 532nm laser is attenuated with a polarizer. The laser is shuttered so that 1-2 pulses are fired. The beam is then expanded to fill the back of a 40x objective on the microscope. Cells were plated on glass bottom poly-l-lysine coated dishes.

2.2 Neuronal Cells and Calcium Biosensor Expression.

Dissociated cortical neurons from E18 rat embryos were plated into 35mm glass-bottom imaging dishes that had been precoated with 0.1% Poly-L-Lysine. Neurons were in plating medium for the first 24 hrs. Plating medium consists of Neurobasal supplemented with 10% fetal bovine serum, 1x B27, and 1x Glutamax from Invitrogen, Carlsbad CA. 24 hours after dissection the medium was replaced with maintenance medium that lacked fetal bovine serum. Half medium replacements were made every other day for both neuronal and cell cultures. On day 6-8, cells were transfected using NeuroMag(OZ Biosciences, San Diego, CA). Experiments were carried out two days after transfection. Commercially available HBSS with 1.8mM Ca^{2+} and HBSS without added Ca^{2+} were utilized for experiments. Cells expressing the Ca^{2+} biosensor were imaged at a distance of 180-275 μm from the edge of their cell body to the laser

focus point. Collected images were analyzed via ImageJ and Metafluor. Shockwave force measurements were done by using a method similar to Rau et al[2].

2.3 Shockwave Force Measurement

A Photron PCI-1024 camera was used to gather images of the bubble dynamics for powers of 190-220µm. The timing of a frame captured during the expansion and collapse of a bubble was subject to jitter of about a microsecond. Thus, averages for radii at specific time points were calculated and fitted by linear interpolation. The bubble wall velocity was calculated using experimental data and then fitted using a bi-exponential model. The shockwave velocity and resultant shear stress profile were inferred via the definite integration of the external fluid velocity profile[11].

3. RESULTS

The laser induced shockwave system was characterized to identify the shear stress cells were subjected to. The maximum bubble size was determined by high-speed imaging and is shown in Figure 2A. Calculated shear stress is shown in Figure 2B. A shaded region is shown between 180-275µm in Figure 2B which depicts the distances that cells were from the laser focus spot upon LIS. At these distances the shear stress encountered by the cells was 5.6-2.4kPa.

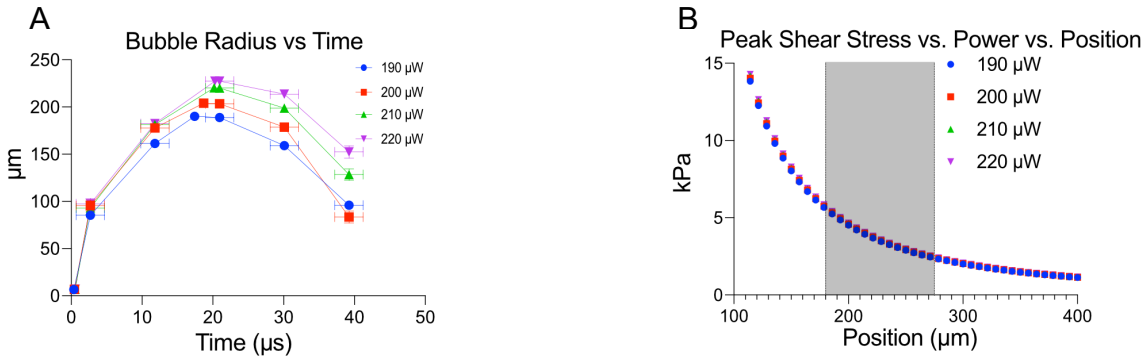

Figure 2. Shockwave system characterization. (A) Bubble radius over time. (B) Peak shear in kPa at different distances from the laser focus. The shaded area depicts the distances that cells were from the focus in our experiments.

Approximately 5% of neurons expressed the Ca^{2+} FRET biosensor. This facilitated our ability to confirm that we were observing a neuron since the axon could be visualized without interference from nearby cells. Upon exposure to shockwave, cells expressing the biosensor demonstrated a transient Ca^{2+} increase that was observed as an increase in the FRET signal and a drop in the ECFP intensity. Ratiometric images were generated in the program MetaFluor which divides the FRET channel by the ECFP channel and assigns a pseudo color to each ratio. Warmer colors indicate greater ratios i.e., greater Ca^{2+}. Figure 3A depicts two cells that were exposed to shockwave whose ratio increases upon shockwave and begins to drop within ~3s after the peak(Figure 3B). The cell depicted by the white arrow(left) appears to have returned to pre-shockwave levels 20s after the peak but continues to drop beyond pre-LIS levels. The cell marked by the yellow arrow had a larger FRET ratio and took longer (~130s) to return to pre-shockwave levels. The normalized FRET ratio F/F_0 is shown in 3B.

An overlay between a pre-LIS phase and a ratiometric image shows the concentric rings that correspond to various radial distances from the laser (Figure 3C). Significant morphological changes were observed in cells closest to the laser focal point when viewed under phase (Figure 3C Post-LIS bottom rectangle and D Post-LIS Bottom). The laser focus was below the field. Therefore, cells on the bottom of the image are closest to the shockwave. Magnifications of enclosed regions in Figure 3C are shown in Figure 3D. Figure 3C top depicts an area further from the shockwave where the cell bodies and processes appear to have retained their morphology; compare pre-LIS top to post-LIS top. An area closest to the shockwave is depicted in pre- and post-LIS Bottom. A cell body is encircled. After LIS, the cell body appears granulated and is no longer recognizable. This cell was ~ 120µm from the laser and would have encountered 10+kPa. Several processes extending from the cell body appear fragmented. A comparison of the calcium response as a

function of distance from the laser demonstrated no significant differences in F/F_o, peak area and time to half maximum of the peak ($T_{1/2}$) when cells were at distances of 180-220µm and 225- 275µm, Figure 3E-G.

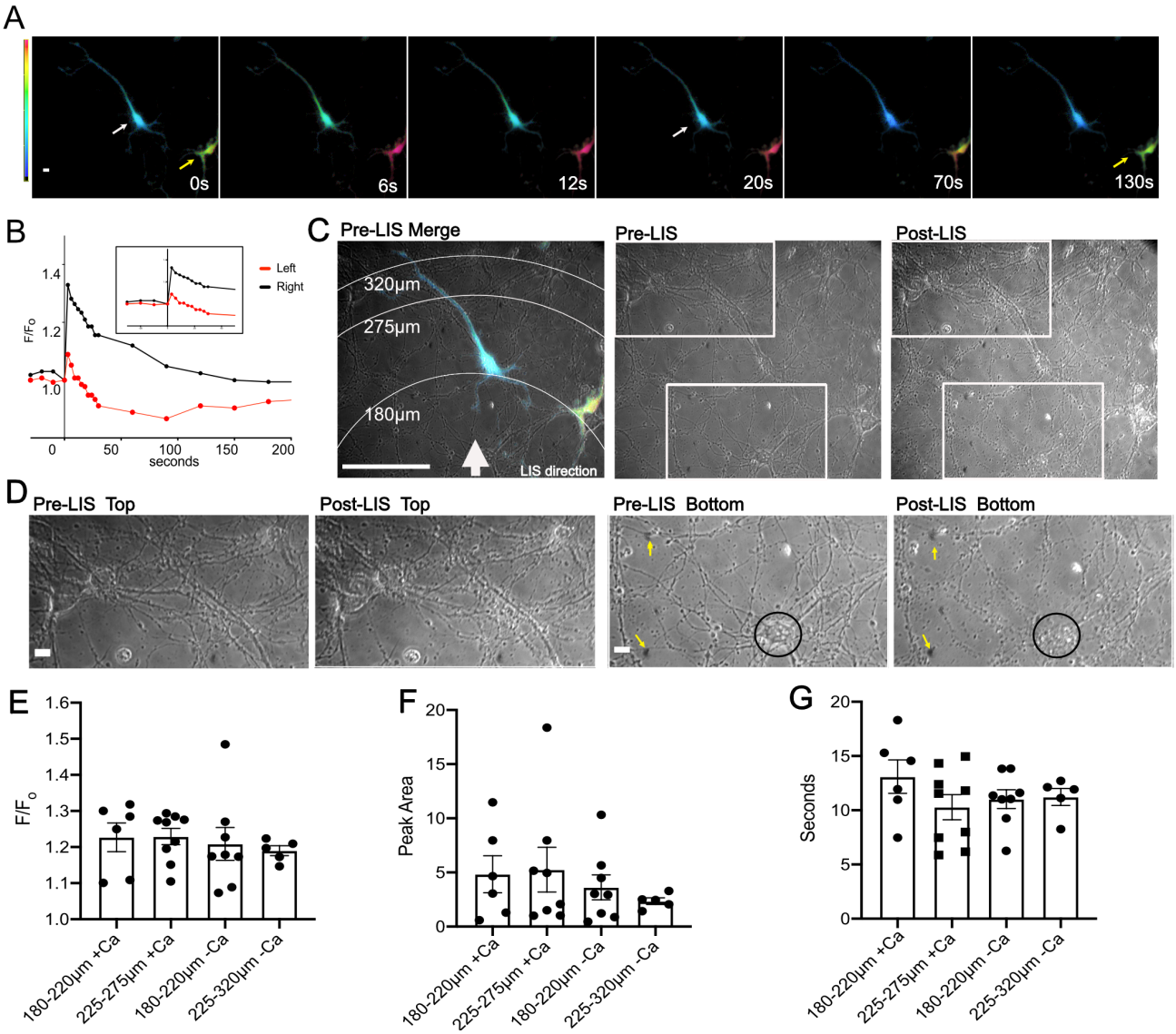

Figure 3. Ratiometric images of two cells that were exposed to LIS. Warmer colors are indicative of a greater FRET ratio i.e. greater Ca^{2+}. A transient increase is observed in both cells. (B) A plot of the F/F_0 of the cells shown in (A). A merge between the phase and ratiometric pre-LIS images is shown in (C) with concentric rings to depict the distances from the laser focus spot. Two phase pre-and post-LIS images to the right have enclosed regions which have been magnified in (D). Cells away from the focus spot, at the top of the image, appear undisturbed; see Pre-LIS Top and Post-LIS Top. Cells closer to the bottom of the field of view appear fragmented, compare Pre-LIS Bottom to Post-LIS Bottom. Yellow arrows indicate immovable objects to demonstrate we are in the same field of view. (E) F/F_o of cells separated by distances and Ca^{2+} availability. +Ca indicates cells bathed in regular (1.8mM) Ca^{2+} conditions. -Ca indicates cells in low calcium conditions. N=6 for 180-220 µm +Ca, N=9 for 225-275 µm +Ca, N=8 for 180-220 µm -Ca, N=5 for 225-275 µm -Ca, except where noted. (F) Peak Area separated by distances. One cell in regular Ca^{2+} and 225-275µm from LIS was excluded from the Peak Area analysis since the F/F_o decreased to a certain point then remained elevated after shockwave causing the peak area to be very high (74 F/F_o*seconds), N=8 for 225-275 µm +Ca. A different cell, outlier in 225-275µm +Ca, reached the half maximum and then remained elevated till t=130s. (G) $T_{1/2}$ of cells separated by distances. No significant differences were found between any comparisons in F/F_o, peak area, and seconds.

The response to shockwave in regular and low Ca^{2+} was averaged and plotted in Figure 4A. The peak response for each condition is compared in Figure 4B. Significant differences are observed between non-shockwaved control cells and cells subjected to shockwave. However, no differences are seen between the peak response at 6s of cells in regular or low calcium which were shockwaved. Similarly, the peak area did not differ in cells under different calcium conditions (Figure 4C).

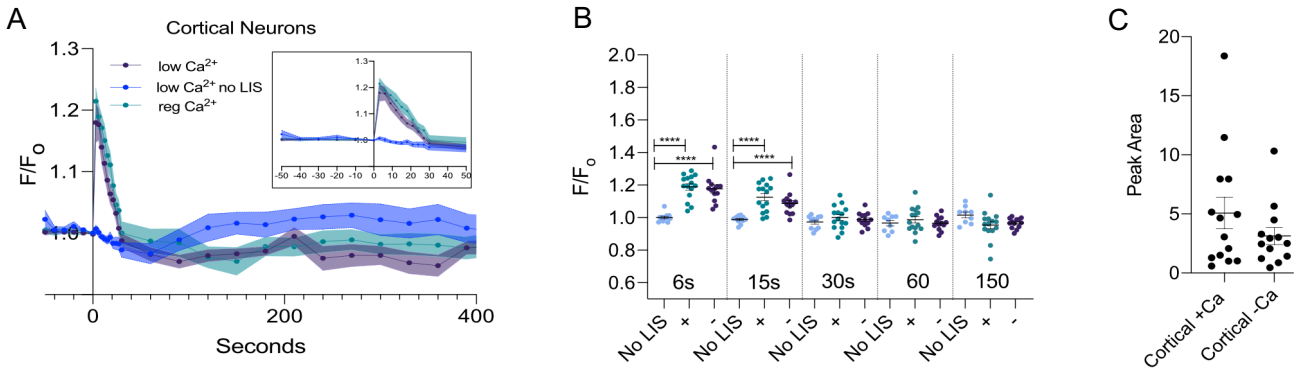

Figure 4. (A) Average F/F_o of cortical neurons in regular Ca^{2+} (teal, n=15 cells) and in low Ca^{2+} (purple, n=13) conditions. Non shockwaved controls were imaged in low Ca^{2+}(blue, n=12). The thickness of each curve is representative of the standard error mean. An inset of the first 50 seconds is shown within the graph. (B) Individual F/F_o values are plotted for cells at 6, 15, 30, 60, and 150 seconds post shockwave. No LIS indicates that cells have not been shockwaved. A plus sign (+) indicates cells were in regular Ca^{2+} Hanks Buffer Saline Solution when shockwaved. A minus sign (-) is used to represent that teezy1
teezcells were in low Ca^{2+} HBSS when shockwaved. Peak values are significantly different between cells receiving LIS and No LIS controls. **** $p \leq 0.0001$, *** $p \leq 0.001$, ** $p \leq 0.01$, * $p < 0.05$. (C) The integral of the time under the transient is shown for cortical cells shockwaved in Ca^{2+} (+Ca) and without (-Ca).. The average area is 5.1 $\pm$ 1.3 (N=14), 3.1 $\pm$ 0.7(N=13).

Interestingly, the confluence of the field of view was found to be correlated to the peak value in cortical cells bathed in regular Ca^{2+} but not for cortical in low Ca^{2+}(Figure 5A). These results suggest that surrounding cells may be influencing Ca^{2+} influx since the correlation was not observed under low Ca^{2+} conditions. However, no relationship was found between confluence and $T_{1/2}$ or Peak Area. Therefore, the overall Ca^{2+} displacement may be similar despite differences in extracellular Ca^{2+} and confluence. Additionally, the FRET ratio before shockwave (F_o) was found to be higher in cells in regular Ca^{2+} compared to cells in low Ca^{2+}(Figure 5B) but no relationship was found between pre-shockwave cytoplasmic Ca^{2+}(F_o) and peak values or $T_{1/2}$ (Figure 5C). Thus, the magnitude of the transient is not likely to be affected by pre-shockwave cytoplasmic Ca^{2+} levels.

Control cells subjected to the same imaging conditions but without shockwave did not show a Ca^{2+} transient like that induced by LIS (Figure 6). Three cells were found to be undergoing a Ca^{2+} decline before t=0s which contributed to the downward slope in the no LIS average, Figure 4A. The increased imaging frequency after t=0 may have further contributed to the decline by inducing photobleaching. Nevertheless, the average F/F_o of control no LIS cells at 6s and 15 seconds is significantly different from those that were shockwaved. This difference disappears at 30s (Figure 4B).

4. DISCUSSION AND CONCLUSIONS

In this study, we demonstrate that cortical neurons respond to LIS with a change in Ca^{2+} ion concentration similar in magnitude irrespective of cell type and availability of Ca^{2+} ions in the bathing culture medium. These results suggest that Ca^{2+} reserves within the cell are largely responsible for the Ca^{2+} ion transient. Curiously, we found a positive correlation between confluence and peak values for cells in regular Ca^{2+} but not for cells in low Ca^{2+}. Therefore, a Ca^{2+} influx may occur at the beginning of the transient in the presence of extracellular Ca^{2+} which is triggered by surrounding cells likely through the release of ATP [12].

Within a distance of 180-275 μm from LIS origination, the calcium transient response did not vary. The peak of the Ca^{2+} transient, duration, and area under the curve did not show significant differences within this distance range. At these distances, the shear stress the cells would have encountered was between 5.6-2.5kPa. Most cells reached the Ca^{2+} peak in the first 6s after LIS. However, further experiments are necessary to determine how lower shear stress because of

being further from the LIS initiation point may affect the Ca^{2+} response. Studies should also be conducted to identify the contents extruded from damaged cells that may be contributing to the Ca^{2+} release in those instances. Nevertheless, the damaging effects of shear stress in neuronal cultures can be studied at different levels using LIS to understand molecular cascades that may occur in TBI. Previous studies have shown that pressure injuries may occur in the range of 10-11.5kPa[13]. With LIS, however, cells can experience shears of 10+kPa at distances up to 120 µm from the laser focal point. At those distances and shear levels, cell fragmentation was observed (Figure 3D Post-LIS Bottom).

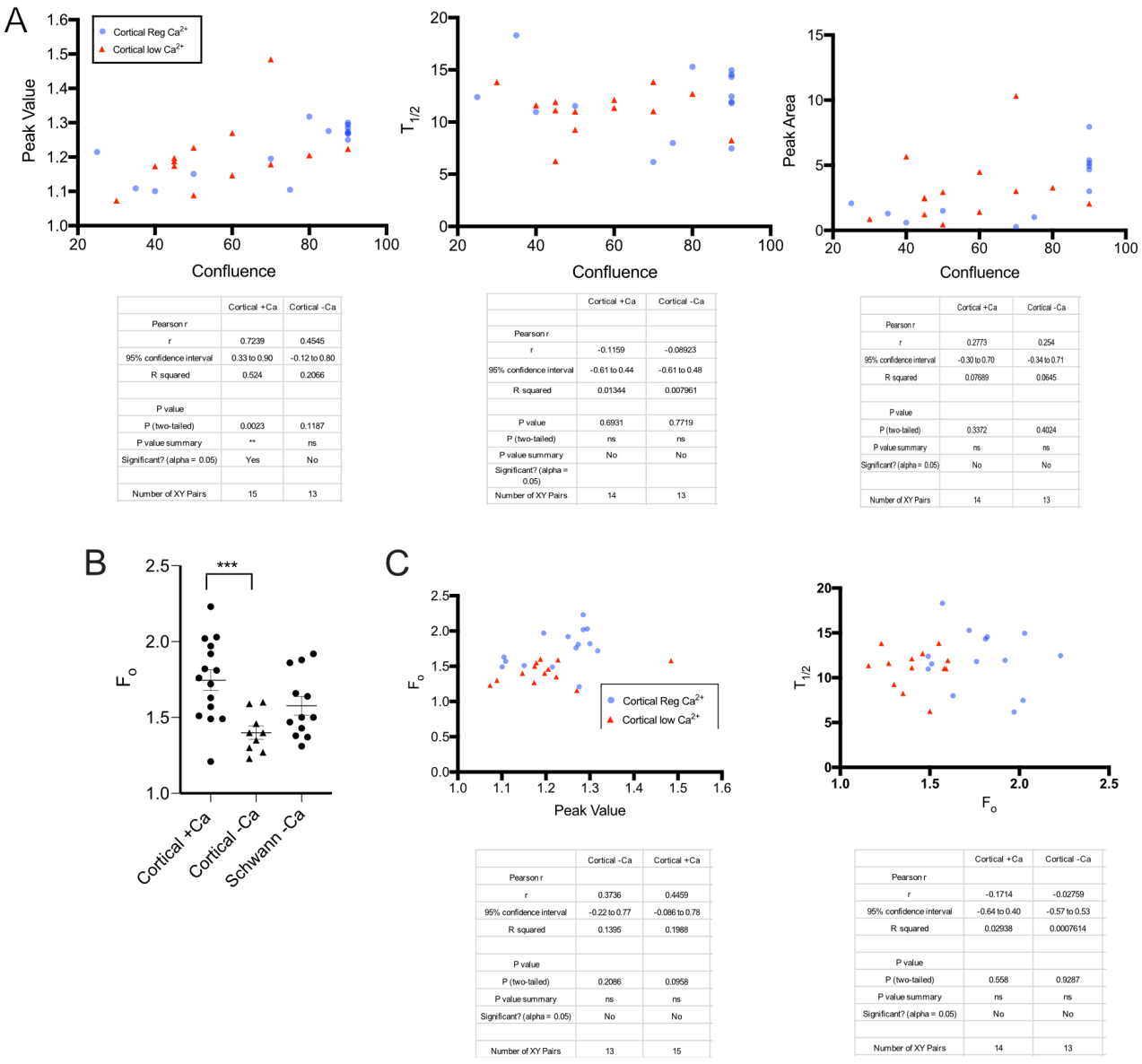

	Cortical +Ca	Cortical -Ca
Pearson r		
r	0.7239	0.4545
95% confidence interval	0.33 to 0.90	-0.12 to 0.80
R squared	0.524	0.2066
P value		
P (two-tailed)	0.0023	0.1187
P value summary	**	ns
Significant? (alpha = 0.05)	Yes	No
Number of XY Pairs	15	13

	Cortical +Ca	Cortical -Ca
Pearson r		
r	-0.1159	-0.08923
95% confidence interval	-0.61 to 0.44	-0.61 to 0.48
R squared	0.01344	0.007961
P value	0.6931	0.7719
P (two-tailed)	ns	ns
P value summary	No	No
Significant? (alpha = 0.05)		
Number of XY Pairs	14	13

	Cortical +Ca	Cortical -Ca
Pearson r		
r	0.2773	0.254
95% confidence interval	-0.30 to 0.70	-0.34 to 0.71
R squared	0.07689	0.0645
P value		
P (two-tailed)	0.3372	0.4024
P value summary	ns	ns
Significant? (alpha = 0.05)	No	No
Number of XY Pairs	14	13

	Cortical -Ca	Cortical +Ca
Pearson r		
r	0.3736	0.4459
95% confidence interval	-0.22 to 0.77	-0.086 to 0.78
R squared	0.1395	0.1988
P value		
P (two-tailed)	0.2086	0.0958
P value summary	ns	ns
Significant? (alpha = 0.05)	No	No
Number of XY Pairs	13	15

	Cortical +Ca	Cortical -Ca
Pearson r		
r	-0.1714	-0.02759
95% confidence interval	-0.64 to 0.40	-0.57 to 0.53
R squared	0.02938	0.0007614
P value		
P (two-tailed)	0.558	0.9287
P value summary	ns	ns
Significant? (alpha = 0.05)	No	No
Number of XY Pairs	14	13

Figure 5. Graphs for correlation analysis. (A) Confluence vs. Peak Value, $T_{1/2}$, and Peak Area. A correlation between confluence in the field of view was found for cortical cells in regular Ca^{2+}. R-squared values and p-values can be found underneath each graph. No correlation was found between confluence and $T_{1/2}$ and Peak Area. (B) F_o for Cortical Cells in regular and low Ca^{2+} (*** $p<0.001$). (C) F_o vs Peak Value and $T_{1/2}$. R squared values and p values can be found underneath each graph.

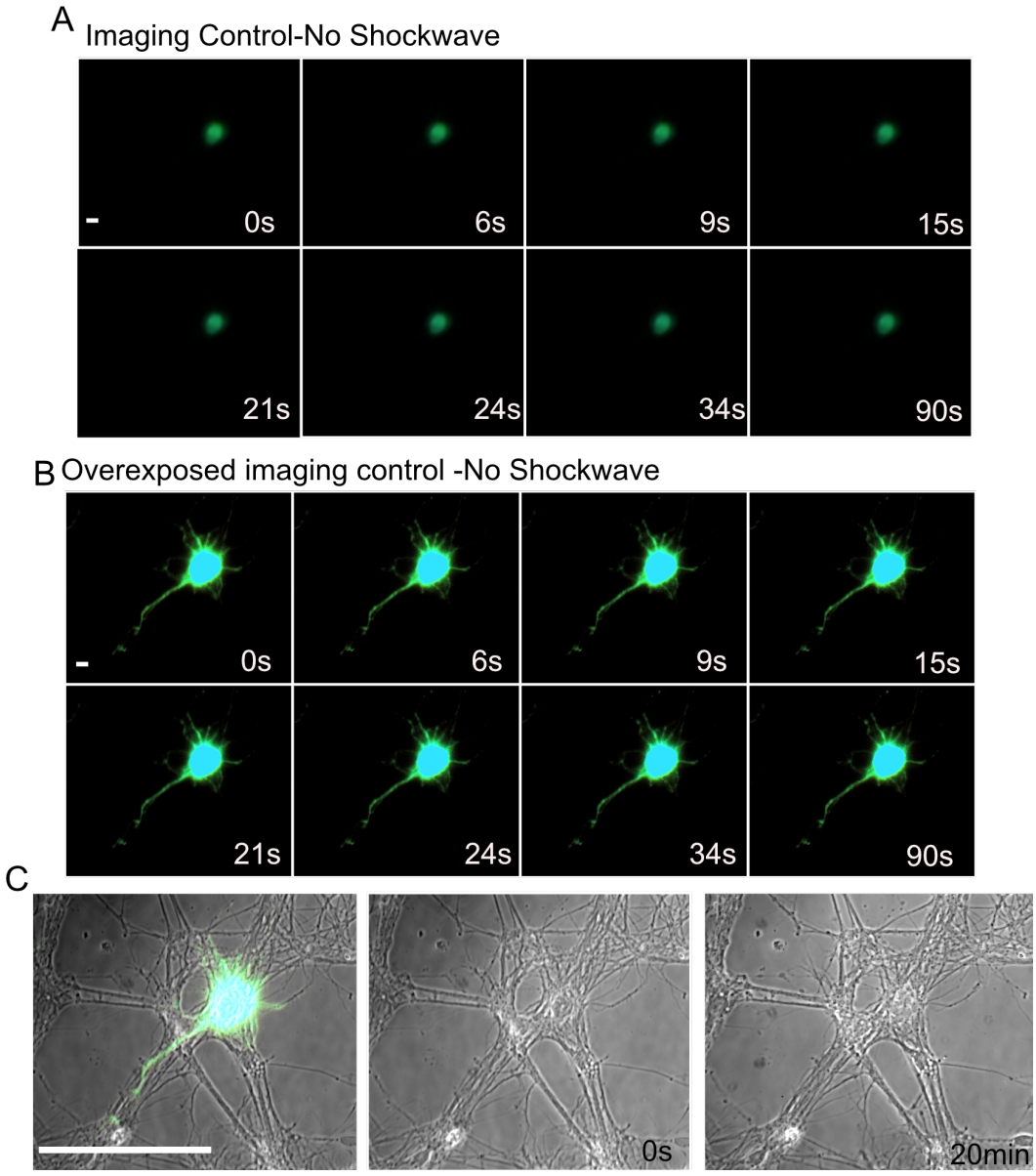

Figure 6. (A) A DIV 9 neuron that is subjected to imaging at the same frequency as cells treated with LIS. Ratiometric images depict unnoticeable changes. Scale bar =10 μm. (B) The same cell as in (A) is shown with the brightness contrast adjusted to show the axon. (C) An overlay between a ratiometric image and phase image is shown. Scale bar= 100μm. Corresponding phase images are shown for cells at 0s and 20min.

The recovery of the cells to pre-shockwave Ca^{2+} concentration levels occurred within the first 30 seconds following exposure to the shockwave. Cortical neurons in low Ca^{2+} medium dropped to lower Ca^{2+} levels than cells in the culture medium with regular extracellular Ca^{2+} levels. These results suggest a contribution of extracellular Ca^{2+} to cytosolic Ca^{2+} levels when the cell returns to pre-shockwave levels. In a previous study using the same shockwave system, we found that bovine arterial cells (BAEC) in low Ca^{2+} HBSS recovered to pre-shockwave levels after the Ca^{2+} transient, but Ca^{2+} levels continued to decrease over time. BAEC cells in regular Ca^{2+} concentrations did not recover to pre-shockwave Ca^{2+} levels; instead, the Ca^{2+} levels remained elevated [5]. Comparing the results of the BAEC cells with the neuronal cells in this study, suggest that the mechanism of recovery likely differs by cell type and the availability of extracellular Ca^{2+}.

While the long-term survival of the neurons was not determined in this study, LIS is a viable method to examine the immediate mechanotransduction and molecular consequences of shockwaves at the cellular level. The proximity of cells to the laser focal point determines the level of shear stress that the cell experiences and the consequent amount of damage produced. This feature makes LIS a useful tool in that the response to shear can be studied in cells that survive and attempt to recover, as well as in cells that progress to cell death. In addition, it will allow the study of cells not exposed to a damaging or lethal LIS-induced shear, but which respond to the release of cytotoxic, purinergic, and other molecular constituents that may affect healthy cells not affected by the LIS.

5. REFERENCES

[1] A. Vogel, W. Hentschel, J. Holzfuss, W. Lauterborn, Cavitation bubble dynamics and acoustic transient generation in ocular surgery with pulsed neodymium: YAG lasers, Ophthalmology, 93 (1986) 1259-1269.

[2] K.R. Rau, P.A. Quinto-Su, A.N. Hellman, V. Venugopalan, Pulsed laser microbeam-induced cell lysis: time-resolved imaging and analysis of hydrodynamic effects, Biophys J, 91 (2006) 317-329.

[3] M.D. Bootman, T.J. Collins, C.M. Peppiatt, L.S. Prothero, L. MacKenzie, P. De Smet, M. Travers, S.C. Tovey, J.T. Seo, M.J. Berridge, F. Ciccolini, P. Lipp, Calcium signalling--an overview, Semin Cell Dev Biol, 12 (2001) 3-10.

[4] V.R. Manuel, S.A. Martin, S.R. Juan, M.A. Fernando, M. Frerk, K. Thomas, H. Christian, Hypocalcemia as a prognostic factor in mortality and morbidity in moderate and severe traumatic brain injury, Asian J Neurosurg, 10 (2015) 190-194.

[5] V. Gomez-Godinez, D. Preece, L. Shi, N. Khatibzadeh, D. Rosales, Y. Pan, L. Lei, Y. Wang, M.W. Berns, Laser-induced shockwave paired with FRET: a method to study cell signaling, Microsc Res Tech, 78 (2015) 195-199.

[6] M. Zhou, E.L. Zhao, H.F. Yang, A.H. Gong, J.K. Di, Z.J. Zhang, Generation of calcium waves in living cells induced by 1 kHz femtosecond laser protuberance microsurgery, Laser Physics, 19 (2009) 1470-1474.

[7] E.K. Shannon, A. Stevens, W. Edrington, Y. Zhao, A.K. Jayasinghe, A. Page-McCaw, M.S. Hutson, Multiple Mechanisms Drive Calcium Signal Dynamics around Laser-Induced Epithelial Wounds, Biophys J, 113 (2017) 1623-1635.

[8] J.L. Compton, J.C. Luo, H. Ma, E. Botvinick, V. Venugopalan, High-throughput optical screening of cellular mechanotransduction, Nat Photonics, 8 (2014) 710-715.

[9] D. Suhr, F. Brummer, U. Irmer, D.F. Hulser, Disturbance of cellular calcium homeostasis by in vitro application of shock waves, Ultrasound Med Biol, 22 (1996) 671-679.

[10] A.E. Palmer, M. Giacomello, T. Kortemme, S.A. Hires, V. Lev-Ram, D. Baker, R.Y. Tsien, Ca2+ indicators based on computationally redesigned calmodulin-peptide pairs, Chemistry & biology, 13 (2006) 521-530.

[11] M. Lokhandwalla, B. Sturtevant, Mechanical haemolysis in shock wave lithotripsy (SWL): I. Analysis of cell deformation due to SWL flow-fields, Physics in medicine and biology, 46 (2001) 413-437.

[12] J. Xia, J.C. Lim, W. Lu, J.M. Beckel, E.J. Macarak, A.M. Laties, C.H. Mitchell, Neurons respond directly to mechanical deformation with pannexin-mediated ATP release and autostimulation of P2X7receptors, The Journal of Physiology, 590 (2012) 2285-2304.

[13] E. Park, J.J. Gottlieb, B. Cheung, P.N. Shek, A.J. Baker, A Model of Low-Level Primary Blast Brain Trauma Results in Cytoskeletal Proteolysis and Chronic Functional Impairment in the Absence of Lung Barotrauma, 28 (2011) 343-357.